Polarization Controller: Angles Configuration and Scattering Properties

Nelson J. Muga[1,2], Armando N. Pinto[1,3], Mário F. Ferreira[2]
[1]Instituto de Telecomunicações, Campus de Santiago, 3810–193 Aveiro – Portugal
Phone: +351 234 377 900, Fax: +351 234 377 901
[2]Departamento de Física, Universidade de Aveiro, Campus de Santiago, 3810–193 Aveiro – Portugal
[3]Departamento de Electrónica, Telecomunicações e Informática, Universidade de Aveiro,
Campus de Santiago, 3810–193 Aveiro – Portugal
E–mails: muga@av.it.pt, anp@det.ua.pt, mferreira@fis.ua.pt

***Abstract* — A detailed study of the relation between the polarization controller angles and its respective polarization scattering properties is presented. First, it is shown that to transform between any two states of polarization the polarization controller angles must be allowed to change, at least, between -π/4 and π/4. After, it is demonstrated that using a concatenation of three polarization controllers, with angles randomly changed between -π/4 and π/4, a uniform polarization scattering over the Poincaré sphere is obtained. Finally, it is analyzed the influence of the configuration angles range and the number of polarization controllers in the scattering properties.**

I. INTRODUCTION

A device or a concatenation of devices, with the ability to produce a uniform polarization scattering over the Poincaré sphere can be useful in the development of polarization mode dispersion (PMD) emulators. Indeed, some authors have proposed PMD emulators, based on pieces of polarization maintaining fibers, interconnected with uniform polarization scattering devices [1]-[3]. The fiber-coil based polarization controller [4] can be used to scatter the state of polarization (SOP) over the Poincaré sphere. In this work, the main scattering properties of this device are analyzed. In particular, it is analyzed the influence of the waveplate angles range in the scattering properties.

II. THE SMALLEST WAVEPLATE PC ANGLES RANGE

The polarization controller (PC) used in this work is schematically represented in Fig. 1. It results from the concatenation of two quarter-waveplates (QWP) and one half-waveplate (HWP), with the last one placed between the other two. To transform an arbitrary input SOP into an also arbitrary output SOP we can do the follow: 1) use the first QWP to transform the input SOP into a linear SOP; 2) use the HWP to change between two linear SOPs; 3) use the second QWP to convert the linear SOP into the desired output SOP. In the following, it is derived the smallest range of waveplate angles, to transform between any given input and output SOP using the method previously described. It is also analyzed the scattering properties of this device considering different angles ranges for the waveplates.

This work was partially supported by the Portuguese Scientific Foundation, FCT, through the "PMD – Polarization Mode Dispersion in High-Speed Optical Communication Systems" project (POSI/CPS/47389/2002), FEDER and POSI programs.

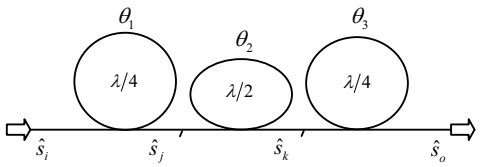

Fig. 1. Schematic representation of the three waveplate polarization controller.

The presented derivation is based on the analysis of the SOP evolution between successive waveplates. The input and output SOPs can be represented, respectively, by the two following Stokes vectors

$$\hat{s}_i = [(s_1)_i, (s_2)_i, (s_3)_i]^T \quad (1)$$

and

$$\hat{s}_o = [(s_1)_o, (s_2)_o, (s_3)_o]^T \quad (2)$$

where T indicates the transpose. In the same way, the SOP after the first and second waveplates (see Fig. 1) can be written, respectively, as

$$\hat{s}_j = [(s_1)_j, (s_2)_j, (s_3)_j]^T \quad (3)$$

and

$$\hat{s}_k = [(s_1)_k, (s_2)_k, (s_3)_k]^T . \quad (4)$$

The SOP after the first waveplate, $\hat{s}_j$, is a function of the input SOP, $\hat{s}_i$, and of the first waveplate angle, θ_1. The respective Stokes vector is [1]

$$\hat{s}_j = \begin{bmatrix} (s_1)_i \cos^2(2\theta_1) + (s_2)_i \cos(2\theta_1)\sin(2\theta_1) + (s_3)_i \sin(2\theta_1) \\ (s_1)_i \cos(2\theta_1)\sin(2\theta_1) + (s_2)_i \sin^2(2\theta_1) - (s_3)_i \cos(2\theta_1) \\ -(s_1)_i \sin(2\theta_1) + (s_2)_i \cos(2\theta_1) \end{bmatrix} . \quad (5)$$

As we are looking to a linear SOP after the first waveplate, the third component of $\hat{s}_j$ should vanishes, which gives the following expression for θ_1,

$$\theta_1 = \frac{1}{2}\arctan\left(\frac{(s_2)_i}{(s_1)_i}\right). \quad (6)$$

Note that when $\hat{s}_i = [0,0,\pm 1]^T$ equation (6) is not defined. This means that for this particular case, and independently of the first waveplate angle, $\hat{s}_j$ is always linear. From (6), we also observe that to change between an arbitrary input SOP and a linear SOP, θ_1 must be allowed to take values between at least $-\pi/4$ and $\pi/4$. Under the condition present in (6), $\hat{s}_j$ can be written as: $\hat{s}_j = [X,Y,0]^T$, where X and Y are given by,

$$X = (s_1)_i \cos^2(2\theta_1) + (s_2)_i \cos(2\theta_1)\sin(2\theta_1) + (s_3)_i \sin(2\theta_1) \quad (7)$$

and

$$Y = (s_1)_i \cos(2\theta_1)\sin(2\theta_1) + (s_2)_i \sin^2(2\theta_1) - (s_3)_i \cos(2\theta_1)\,. \quad (8)$$

In a similar way, the linear SOP at the end of the second waveplate, the HWP, can be represented as $\hat{s}_k = [W,Z,0]^T$: note that the two non null vector components, W and Z, are functions of the output SOP. The two linear SOPs, $\hat{s}_j$ and $\hat{s}_k$, are related by the following HWP-induced SOP rotation,

$$\hat{s}_k = \boldsymbol{R}(\theta_2)\boldsymbol{M}_{\lambda/2}\boldsymbol{R}(-\theta_2)\hat{s}_j \quad (9)$$

where the matrices $\boldsymbol{M}_{\lambda/2}$ and $\boldsymbol{R}$ represent, in the Stokes space, the HWP and its principal axes orientation [1], respectively. After matrices multiplication, (9) can be written as:

$$\begin{bmatrix} W \\ Z \\ 0 \end{bmatrix} = \begin{bmatrix} (2\cos^2(2\theta_2)-1)X + 2\cos(2\theta_2)\sin(2\theta_2)Y \\ 2\cos(2\theta_2)\sin(2\theta_2)X + (1-2\cos^2(2\theta_2))Y \\ 0 \end{bmatrix}. \quad (10)$$

Using the two first equations of (10), the HWP angle, θ_2, can be expressed as a function of X, Y, W and Z,

$$\theta_2 = \frac{1}{2}\arctan\left(\frac{Y+Z}{X+W}\right). \quad (11)$$

Analogously to θ_1, also θ_2 must be allowed to take values between $-\pi/4$ and $\pi/4$. Note that, in this case, the waveplate angle is a function of both input and output SOPs. The SOP after the third waveplate, $\hat{s}_o$, is obtained applying the rotation matrices $\boldsymbol{R}(\theta_3)\boldsymbol{M}_{\lambda/4}\boldsymbol{R}(-\theta_3)$ to $\hat{s}_k$, where $\boldsymbol{M}_{\lambda/4}$ represents the QWP,

$$\begin{bmatrix} (s_1)_o \\ (s_2)_o \\ (s_3)_o \end{bmatrix} = \begin{bmatrix} W\cos^2(2\theta_3) + Z\cos(2\theta_3)\sin(2\theta_3) \\ W\cos(2\theta_3)\sin(2\theta_3) + Z\sin^2(2\theta_3) \\ -W\sin(2\theta_3) + Z\cos(2\theta_3) \end{bmatrix}. \quad (12)$$

The expression for the third waveplate angle is obtained using the two first equations of (12), and solving them in order to θ_3,

$$\theta_3 = \frac{1}{2}\arctan\left(\frac{(s_2)_o}{(s_1)_o}\right). \quad (13)$$

Using the first and third equations of (12), in conjugation with (13), the following expression is founded to W,

$$W = (s_1)_o \cos^2(2\theta_3) + (s_2)_o \cos(2\theta_3)\sin(2\theta_3) - (s_3)_o \sin(2\theta_3). \quad (14)$$

In the same way, using the second and third equations of (12), in conjugation with (13), the following expression is founded for Z,

$$Z = (s_1)_o \cos(2\theta_3)\sin(2\theta_3) + (s_2)_o \sin^2(2\theta_3) + (s_3)_o \cos(2\theta_3). \quad (15)$$

With the help of these two equations, (14) and (15), the three waveplate angles can be, explicitly, represented as functions of the input and output SOPs. From (6), (11) and (13) we conclude that to transform an arbitrary input SOP into an also arbitrary output SOP the three waveplate angles must be allowed to change at least in the range $-\pi/4$ to $\pi/4$. We also conclude that, following the three steps method (arbitrary input SOP, linear SOP, linear SOP and arbitrary output SOP), this is the smallest waveplate angles range to perform the change between any two SOPs.

III. POLARIZATION SCATTERING

To scatter the SOP a concatenation of several PCs is considered. The SOP at the nth PC output, $\hat{s}_{n+1}$, is related with the SOP at the nth PC input, $\hat{s}_n$, by the following expression,

$$\hat{s}_{n+1} = \boldsymbol{F}\,\hat{s}_n\,. \quad (16)$$

The matrix $\boldsymbol{F}_n(\theta_{1,n},\theta_{2,n},\theta_{3,n})$ represents the nth PC (see Fig. 2), resulting from the concatenation of three waveplates (QWP – HWP – QWP) with principal axes orientation given by $\theta_{1,n}$, $\theta_{2,n}$ and $\theta_{3,n}$.

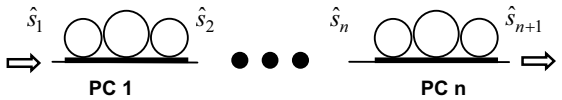

Fig. 2. Schematic representation of a concatenation of n PCs and respective input and output SOPs.

We are going to assume that the PC angles are randomly changed, following a uniform distribution between $-m\pi/4$ and $m\pi/4$, where m is a positive integer number. We are also going to assume that the change is independent between the angles of waveplates of the same PC and between the angles of waveplates of different PCs. Therefore, the average value of the $\boldsymbol{F}$ matrix elements, f_{ij}, will be equal for all the n PCs and will be hereafter designated simply by $< f_{ij} >$. The average values of the $\boldsymbol{F}$ matrix elements, calculated as in [1], are

$$\left\langle f_{ij} \right\rangle_{\theta_i \in [-m\frac{\pi}{4};m\frac{\pi}{4}]} = \delta_{2i}\ \delta_{2j}\ \delta_{1(-1)^{m-1}}\frac{4}{(m\pi)^2}, \qquad (17)$$

where δ_{ij} is the Kronecker delta. Note that $< f_{22} >$ only vanishes if m is an even number. When m is an odd number, $< f_{22} >$ do not vanish, but converges to zero as m increases: this evolution is graphically represented in Fig. 3.

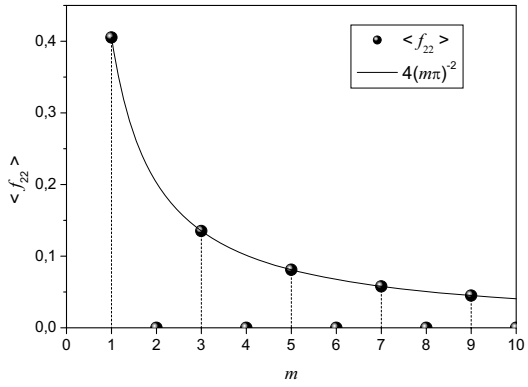

Fig. 3. Evolution of the f_{22} mean value as function of the parameter m (marks). Solid line represents the evolution of f_{22} mean value when m is an odd number.

Using (17) into (16), and using (16) iteratively for an arbitrary initial SOP $\hat{s}_1 = [(s_1)_1, (s_2)_1, (s_3)_1]^T$, the mean values of the Stokes vector components, at the end of the nth PC, $< \hat{s}_{n+1} >$, are obtained,

$$\begin{bmatrix} \langle (s_1)_{n+1} \rangle \\ \langle (s_2)_{n+1} \rangle \\ \langle (s_3)_{n+1} \rangle \end{bmatrix}_{\theta_i \in [-m\frac{\pi}{4};m\frac{\pi}{4}]} = \delta_{1(-1)^{m-1}}(s_2)_1 \frac{1}{\left(\frac{(m\pi)^2}{4}\right)^n}\begin{bmatrix} 0 \\ 1 \\ 0 \end{bmatrix} + \delta_{n0}(s_2)_1\left(1-\delta_{1(-1)^{m-1}}\frac{4}{(m\pi)^2}\right)\begin{bmatrix} 0 \\ 1 \\ 0 \end{bmatrix} \qquad (18)$$

where m defines the width of the waveplates angle variation range. On the other hand, all mean square values of the Stokes vector components are independent of m, and are given by [1]

$$\begin{bmatrix} \langle (s_1)_{n+1}^2 \rangle \\ \langle (s_2)_{n+1}^2 \rangle \\ \langle (s_3)_{n+1}^2 \rangle \end{bmatrix} = \frac{1}{3}\begin{bmatrix} 1 \\ 1 \\ 1 \end{bmatrix} + \frac{a}{4^n}\begin{bmatrix} 1 \\ 1 \\ -2 \end{bmatrix} + \delta_{n0}b\begin{bmatrix} 1 \\ -1 \\ 0 \end{bmatrix} \qquad (19)$$

where a and b are functions of the initial SOP, $\hat{s}_1$,

$$a = \frac{1}{2}\left(\frac{1}{3} - (s_3)_1^2\right) \qquad (20)$$

and

$$b = \frac{1}{2}\left((s_1)_1^2 - (s_2)_1^2\right). \qquad (21)$$

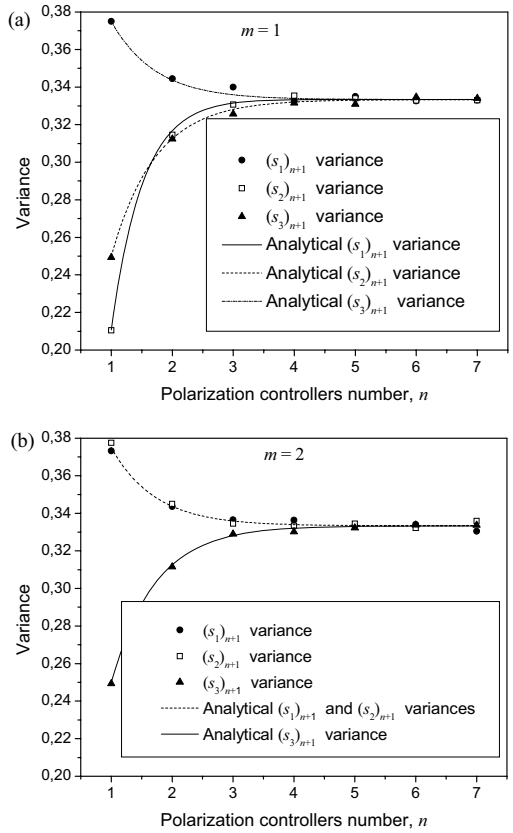

Fig. 4. Variances evolution as function of the number of concatenated PCs, (a) m=1; (b) m=2. Analytical values are represented as lines, whereas simulated values are represented as symbols.

The variances for each Stokes vector component, at the end of the nth PC, are given by

$$\sigma^2(s_i) = \left\langle (s_i)_{n+1}^2 \right\rangle - \left\langle (s_i)_{n+1} \right\rangle^2. \qquad (22)$$

In Fig. 4(a) and Fig. 4(b) are represented, respectively, the variances for the cases m=1 and m=2, considering a particular initial SOP $\hat{s}_1 = [0,1,0]^T$. In both cases the variance converges to the value 1/3: this is the theoretical value for a uniform distribution of SOPs over the Poincaré sphere. Note that, if we have a uniform distribution of points over the Poincaré sphere, each Stokes vector component has a uniform distribution between -1 and 1 [1]. From (18) and (19), in conjugation with the results presented in Fig. 4, we can conclude that the best waveplates angles range to scatter the polarization is $-\pi/2$ to $\pi/2$. In this case all mean values $<(s_i)_{n+1}>$ vanish and $<(s_i)^2_{n+1}>$ converges rapidly to the 1/3 value when the number of PCs increases.

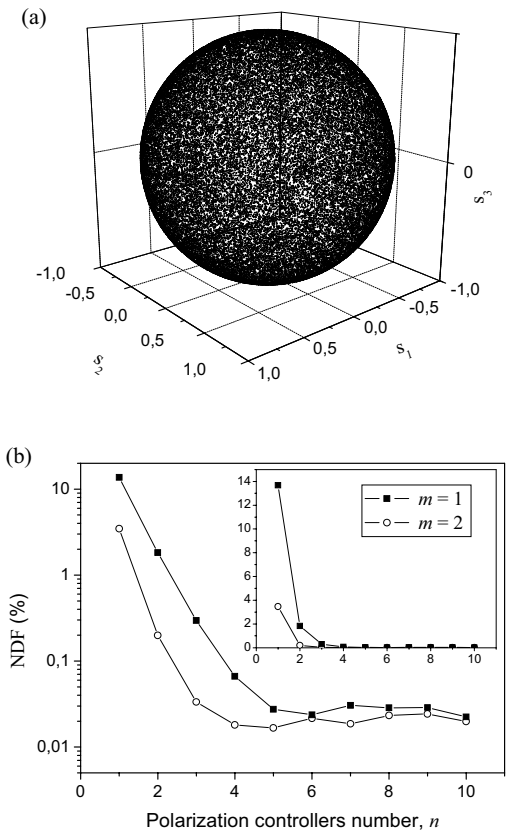

Fig. 5. (a) Poincaré sphere representation of the output SOPs for an initial SOP $\hat{s}_1 = [0,1,0]^T$, n=4 and m=2; (b) sum of Stokes vector component distribution NDFs as function of the PCs number. Inset shows the plot in a normal scale.

In order to validate the theoretical results, with respect to the influence of waveplate angles range on the scattering properties, we have simulated 50000 SOP scatterings. A concatenation of four PCs, with m=2, and an initial SOP $\hat{s}_1 = [0,1,0]^T$ were used to obtain each SOP. As represented in Fig. 5(a), a good uniform distribution of points over the Poincaré sphere is observed. To quantify the influence of the number of PCs, n, and the angles range parameter, m, on the uniformity of the scattering we calculate, for each Stokes vector component distribution, $p_{(s_i)}$, a Normalized Deviation Factor (NDF) [2]. In Fig. 5(b) is represented the sum of the three Stokes vector component distribution NDFs as function of the concatenated PCs number, for the cases m=1 and m=2. Results show that with m=2 uniform distributions can be achieved using a lower number of PCs, when compared with the ones obtained with m=1. Nevertheless, for six or more concatenated PCs we observe that the uniformity degree of the obtained distributions is similar.

IV. CONCLUSIONS

To transform the light state of polarization between any two polarization states, using a PC device, the configuration angles must be allowed to change at least between $-\pi/4$ and $\pi/4$. By changing randomly the configuration angles between $-\pi/4$ and $\pi/4$ it is possible to obtain a uniform polarization scattering concatenating at least three PCs devices. A slightly improvement in the scattering properties can be obtained if the configuration angles are allowed to change between $-\pi/2$ and $\pi/2$.

REFERENCES

[1] N. J. Muga, A. N. Pinto, M. F. S. Ferreira, J. R. F. da Rocha, 'Uniform Polarization Scattering With Fiber-Coil-Based Polarization Controllers', *IEEE/OSA J. Lightwave Technol.*, vol. 24, n.11, pp. 3932–3943, November, 2006.

[2] Y. K. Lizé, L. Palmer, N. Godbout, S. Lacroix, R. Kashyap, 'Scalable Polarization-Mode Dispersion Emulator With Proper First- and Second-Order Statistics', *IEEE Photonics Technol. Lett.*, vol. 17, no. 11, pp. 2451–2453, November, 2005.

[3] I. T. Lima, R. Khosravani, P. Ebrahimi, E. Ibragimov, C. R. Menyuk, A. E. Willner, 'Comparison of Polarization Mode Dispersion Emulators', *IEEE/OSA J. Lightwave Tech.*, vol. 19, no. 12, pp. 1872–1881, December, 2001.

[4] H. C. Lefevre, 'Single-mode Fibre Fractional Wave Devices and Polarization Controllers', *Electron. Lett.*, vol. 16, no. 20, pp. 778–780, September, 1980.